Five-dimensional structure refinement of decagonal $Al_{78}Mn_{22}$

1991 J. Phys.: Condens. Matter 3 3397

(http://iopscience.iop.org/0953-8984/3/20/001)

J. Phys.: Condens. Matter 3 (1991) 3397–3410. Printed in the UK

Five-dimensional structure refinement of decagonal $Al_{78}Mn_{22}$

W Steurer
Institut für Kristallographie und Mineralogie der Universität, Theresienstraße 41, D-8000 München 2, Federal Republic of Germany

Received 23 May 1990, in final form 24 January 1991

Abstract. A single-crystal x-ray structure analysis of the metastable decagonal phase $Al_{78(2)}Mn_{22(2)}$, centrosymmetric superspace group $P10_5/mmc$, has been performed using the n-dimensional (n-D) approach. The structure has been solved by Patterson analysis and subsequent least-squares refinement, both in the 5D description. The final $wR = 0.144$ for 233 independent reflections with $I > 2\sigma(I)$ and 18 variables. There are four 5D atoms in the asymmetric unit generating one planar and one strongly puckered quasiperiodic atomic layer in physical space. These layers show close resemblance to the respective planar and puckered layers of the crystalline $Al_{13}Fe_4$ phase. The 3D decagonal structure is built of periodically stacked packings of six such layers per translation period.

1. Introduction

The present paper is the third in a series of single-crystal x-ray-diffraction studies of decagonal $Al_{78(2)}Mn_{22(2)}$. The first reports a reciprocal-space study using film techniques (Steurer and Mayer 1989; in the following referred to as paper I), the second gives the results of a 5D Patterson analysis, demonstrating the layer structure and deriving a 5D structure model fo the decagonal phase (Steurer 1989; in the following referred to as paper II). To the knowledge of the author, these two papers are the only published single-crystal x-ray studies of decagonal $Al_{78}Mn_{22}$, possibly due to the problem of obtaining sufficiently large single crystals of this metastable phase. There are, however, a large number of papers reporting structural studies with other methods such as electron diffraction, x-ray powder diffraction or spectroscopical techniques. A detailed review of this work is given in paper II and in the review article of Steurer (1990), and shall not be repeated in the present paper, which has the aim of transforming the qualitative structure model of paper II into a quantitative one by 5D least-squares structure refinement. The main motivation for these 5D refinements was to obtain the signs of structure factors for the calculation of 3D Fourier syntheses, which represent directly the electron-density distribution function of decagonal $Al_{78}Mn_{22}$. It should be kept in mind, however, that the diffuse scattering described in paper I is not considered in the present study. The Bragg reflections alone contain information of an average structure only, which will result in an at least partially statistical character of the 5D atoms and/or some smeared 5D density regions.

2. How to perform a quasicrystal structure analysis

Quasicrystals can be recognized easily by their diffraction patterns, which show sharp Bragg reflections in an arrangement with non-crystallographic point symmetry (icosahedral, decagonal,...). Non-crystallographic point symmetry operations, like a fivefold rotation, for instance, are not compatible with a 3D periodic translation lattice. They can, however, become compatible with a n-D space lattice, if the dimension n of the lattice is chosen in an appropriate way (Levitov and Rhyner 1988). Therefore, a structure which is quasiperiodic in 3D can be described as a periodic structure in n dimensions, as was first suggested by de Wolff (1974) for incommensurately modulated phases and by Janssen (1966) for quasicrystals. For the n-dimensional embedding method, the 3D diffraction pattern (quasiperiodic reciprocal lattice) is considered to be a projection of an n-D diffraction pattern (periodic reciprocal lattice) upon physical space. Since direct and reciprocal spaces are connected by a Fourier transformation, a projection in reciprocal space corresponds to a section in direct space and *vice versa*. Thus, the 3D quasiperiodic structure represents an irrational hyperplane of a fictitious n-D supercrystal.

What is the main advantage of a n-D description (with n-D unit cells building the periodic n-D translation lattice) compared with any 3D one? The tools of regular crystal structure analysis are all based on the unit-cell approach, i.e. symmetry, metrics and content of one single unit cell are representative of the structure of the whole crystal. Thus, classical techniques like Patterson and Fourier synthesis or direct methods can be employed for n-D quasicrystal structure analysis in an extended form again. The aim of such a structure determination is to find where the atoms are in the real 3D quasicrystal. The n-D approach represents an intermediate state in the handling of structural information, between 3D diffraction data and 3D quasicrystal structure information. In addition, the n-D description allows a clearer comparison of the structural differences of different quasicrystal structures.

The task of the n-D least-squares refinements is to optimize a qualitative n-D start model. The parameters defining the location, shape, scattering power, thermal vibrations and/or statistical disorder are varied to give the best fit of observed and calculated diffraction intensities. In the case of low quality quasicrystals in particular, one has to confine oneself to a very limited number of free variables leading to a first approximation of the n-D atoms only. As in regular structure analysis, however, a subsequent Fourier synthesis performed with calculated phases and observed structure amplitudes yields additional information: atoms not included in the refinement of the structure model appear in the Fourier maps, smeared electron density due to disorder is located, etc. Thus, at the end of each structure analysis the n-D and 3D Fourier maps should be plotted, to derive all valuable information which is not included in the structure model but is hidden in the diffraction data. The 3D Fourier maps give the answer to the question of where the atoms are directly, and from the height of the maxima in the layer-line plots, the type of atoms can be derived (for x-rays Mn peaks are expected to be two times stronger than Al maxima).

A detailed analysis of the symmetry and metrics of decagonal $Al_{78(2)}Mn_{22(2)}$, and the method of indexing the Bragg reflections was given in paper I. The information necessary for the understanding of the coordinate systems used for the unit-cell description and for the 5D Patterson and Fourier synthesis is represented graphically in figure 1. The 5D embedding space $\mathcal{V}$ consists of two orthogonal subspaces, the 3D external (physical, parallel) space $\mathcal{V}_E$, with the orthogonal basis vectors $\boldsymbol{v}_1$, $\boldsymbol{v}_2$ and $\boldsymbol{v}_3$, and the 2D internal (complementary, perpendicular) space $\mathcal{V}_I$, with orthogonal basis vectors $\boldsymbol{v}_4$ and $\boldsymbol{v}_5$. All

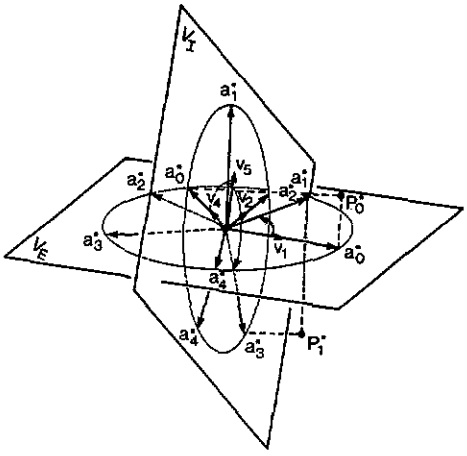

Figure 1. Schematical representation of the orthogonal subspaces $\mathcal{V}_E$, spanned by the basis vectors $\boldsymbol{v}_1$, $\boldsymbol{v}_2$ ($\boldsymbol{v}_3$ was not drawn for reasons of clarity), and $\mathcal{V}_I$ with basis vectors $\boldsymbol{v}_4$ and $\boldsymbol{v}_5$. $\mathcal{V}_E$ and $\mathcal{V}_I$ intersect each other in one single point only: the origin of the basis vectors. The projections of the 5D basis $\boldsymbol{d}_i$ upon $\mathcal{V}_E$ and $\mathcal{V}_I$, the vectors $\boldsymbol{a}_i^*$, are marked. The transformation of a point P_0^* given by its 5D coordinates $(\boldsymbol{a}_0^*, 0, \boldsymbol{a}_0^*)$ by a five-fold rotation onto P_1^* with $(\boldsymbol{a}_1^*, 0, \boldsymbol{a}_3^*)$ corresponds to a rotation through an angle of $2\pi/5$ in $\mathcal{V}_E$, and one through $6\pi/5$ in $\mathcal{V}_I$.

reciprocal lattice vectors of each quasiperiodic reciprocal lattice layer spanned by $\boldsymbol{v}_1$ and $\boldsymbol{v}_2$ in $\mathcal{V}_E$ can be represented by linear combinations of five basis vectors pointing to the corners of a regular pentagon $\boldsymbol{a}_i^* = a_i^*(\cos 2\pi i/5, \sin 2\pi i/5, 0)$ with $i = 0, \ldots, 4$, and $\boldsymbol{a}_0^* = -(\boldsymbol{a}_1^* + \boldsymbol{a}_2^* + \boldsymbol{a}_3^* + \boldsymbol{a}_4^*)$, forming a symmetry-adapted basis. Perpendicular to the plane formed by this and parallel to the tenfold axis, a further reciprocal basis vector $\boldsymbol{a}_5^* = a_5^*(0, 0, 1)$ parallel to $\boldsymbol{v}_3$ is required. The star of the five vectors in the $(\boldsymbol{v}_1, \boldsymbol{v}_2)$—plane which corresponds to the projection of the 5D reciprocal basic vectors $\boldsymbol{d}_i^* = (\boldsymbol{a}_i^*, 0, \boldsymbol{a}_{3i}^*)$, $i = 1, \ldots, 4$ upon $\mathcal{V}_E$ is shown in figure 1. The star in the $\mathcal{V}_I$ plane results consequently from the projection upon $\mathcal{V}_I$. The action of a fivefold rotation in 5D space, as it is defined by its matrix representation given in paper II, is also given in figure 1. By the action of this 5-fold symmetry operation, the point P_0^* with 5D coordinates $(\boldsymbol{a}_0^*, 0, \boldsymbol{a}_0^*)$, for instance, is transformed into P_1^* with $(\boldsymbol{a}_1^*, 0, \boldsymbol{a}_3^*)$. The projection of the trajectory upon $\mathcal{V}_E$ and $\mathcal{V}_I$ corresponds to rotation components of $2\pi/5$ and $6\pi/5$, respectively. For the description of the 5D unit cell we use the $\boldsymbol{d}_i$ basis; for the discussion of the characteristic features of the internal and external spaces the $\boldsymbol{v}_i$ basis is more appropriate.

3. Experiment

A detailed description of the preparation of a single crystal of metastable decagonal $Al_{78(2)}Mn_{22(2)}$, its investigation by x-ray photographic techniques and the indexing of reflections was given in paper I. The reflections are quite broad, the average FWHMs are at least four times larger than those which are observed in the case of normal crystals on our diffractometer. Nevertheless, a remarkable number of reflections with large internal components of the diffraction vector are observable (cf. figure 2 of paper II). The crystals of the decagonal phase underwent a phase transformation, at room temperature, to amorphous material within one year of their preparation. X-ray photographs showed powder rings and diffuse scattering, only. This is one additional argument that the crystal investigated was a metastable quasicrystal and not a multiply twinned regular crystal.

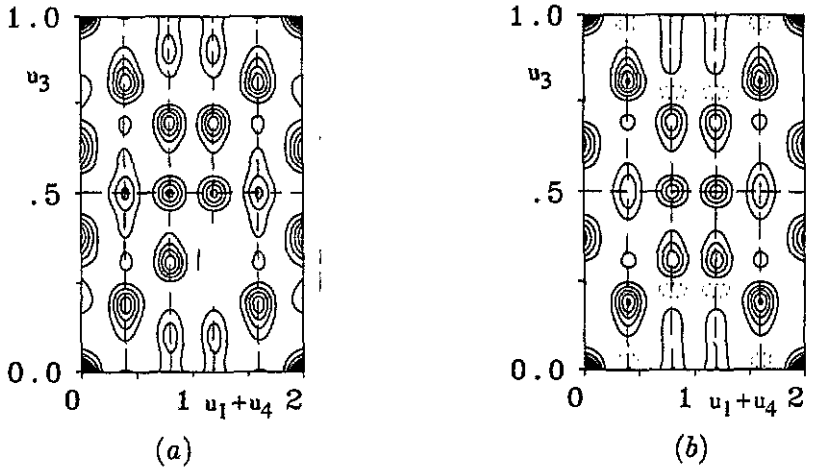

Figure 2. A characteristic (10110) section of the 5D Patterson function: (*a*) intensities computed from observation and (*b*) calculated intensities. All maxima of one unit cell are contained in this plane. All plot coordinates are given on the v_i basis.

3.1. Data collection

The x-ray equipment used was an Enraf-Nonius CAD4 four-circle diffractometer, with Mo$K\alpha$ radiation and a graphite monochromator. Lattice parameters were refined from 24 reflections. ω-scans with $\omega = 5.0 + 0.35 \tan \theta^0$, extended at each side by 25% for background determination. Out of the infinite number of possible reflections within $0 < \theta < 30°$ in a first run, all those within one asymmetric unit were measured with $-3 < h_i < 3, i = 1$ to 4, and $0 < h_5 < 17$. This data set includes all reflections observable on the x-ray precession photographs. A denser set of reflections may give resolution problems and would not yield much more observable intensities since it is known that the geometrical form factor g_k causes a rapid decrease of the intensities with increasing internal component of the diffraction vector. In this way, 1807 intensities were collected with constant scan time of 4 min/reflection. The 332 reflections of this data set with $1 > 2\sigma(I)$ ($\sigma(I)$: standard deviation from counting statistics) were remeasured in ten symmetrically equivalent asymmetric units with a scan time of 4 min/reflection. The full set of 5189 intensities was corrected for Lorentz and polarization effects but not for absorption (due to the very irregular shape of the crystal). After rejecting the weakest and the strongest reflections of each symmetrically equivalent set, the arithmetic mean and its standard deviation was calculated from the—at least eight—remaining intensities. ($R_i = 0.038$, 233 unique reflections with $I > 2\sigma(I)$).

4. Structure solution and refinement

The structure of decagonal $Al_{78(2)}Mn_{22(2)}$ has been solved in a rather straightforward manner. The 5D Patterson function (figure 2 (a)) is easy to interpret and a model with three atoms in the asymmetric unit has been used as the starting set for the least-squares refinements of the 5D structure. The function minimized was

$$\chi^2 = \Sigma\, w_i(|F_{obs}(H)| - |F_{clc}(H)|)^2$$

with observed and calculated structure amplitudes $|F_{obs}(\boldsymbol{H})|$, $|F_{clc}(\boldsymbol{H})|$, respectively, and with weights $w_i = k/\sigma^2(F(\boldsymbol{H}))$; k is refined to obtain $\chi^2 = 1$. This is recommended in all cases in which the errors of the reflection intensities are larger than is expected by counting statistics alone (Prince 1982). The reliability factors R and wR used were

$$R = \left(\sum ||F_{obs}(\boldsymbol{H})| - |F_{clc}(\boldsymbol{H})||\right)\left(\sum |F_{obs}(\boldsymbol{H})|\right)^{-1}$$

$$wR = \left[\sum w_i(|F_{obs}(\boldsymbol{H})| - |F_{clc}(\boldsymbol{H})|)^2 \left(\sum w_i |F_{obs}(\boldsymbol{H})|^2\right)^{-1}\right]^{1/2}.$$

The structure factor formula applied in the refinements was

$$F(\boldsymbol{H}) = 1/\Omega_I \sum_k \exp(2\pi i \boldsymbol{H}\cdot\boldsymbol{r}_k) f_k(\boldsymbol{H}_E) p_k T_k(\boldsymbol{H}_E, \boldsymbol{H}_I) g_k(\boldsymbol{H}_I)$$

with diffraction vector $\boldsymbol{H} = (\boldsymbol{H}_E, \boldsymbol{H}_I) = \Sigma_i h_i \boldsymbol{d}_i^*$, $i = 1, 5$. On the $\boldsymbol{v}_i$ basis the components of the diffraction vector are defined as $\boldsymbol{H}_E = h_1^E \boldsymbol{v}_1^* + h_2^E \boldsymbol{v}_2^* + h_3^E \boldsymbol{v}_3^*$ and $\boldsymbol{H}_I = h_4^I \boldsymbol{v}_4^* + h_5^I \boldsymbol{v}_5^*$. The positional vector of the atom k is given by $\boldsymbol{r}_k = \Sigma_i x_i^k \boldsymbol{d}_i$. The atomic scattering factor $f_k(\boldsymbol{H}_E)$ depends on the external component of the diffraction vector, only. p_k is the occupancy factor, the temperature factor $T_k(\boldsymbol{H}_E, \boldsymbol{H}_I)$ is written in the form

$$T_k(\boldsymbol{H}_E, \boldsymbol{H}_I) = \exp\{-\tfrac{1}{4}[B_{11}^E(h_1^{E2} + h_2^{E2})a_1^{*2} + B_{33}^E h_3^{E2} a_5^{*2}] + B^I(h_4^{I2} + h_5^{I2})a_1^{*2}\}.$$

It contains the isotropic in-plane term B_{11}^E and the perpendicular component B_{33}^E, both in external space, as well as one coefficient B^I in internal space. The external temperature factor components of the 5D atoms have the same meaning as the temperature factor of a regular structure. The internal component, corresponding to a smearing of the 5D atom parallel to internal space, leads to a higher frequency of intersections of 5D atoms with the physical space. Hence, a number of interstitial sites become occupied at the cost of the regular ones. Displacive disorder may, therefore, be described by the external and substitutional disorder by the internal part of the temperature factor. The geometrical form factor is given by

$$g_k(\boldsymbol{H}_I) = (1/a^*)^2 \sum_j \sin\theta_{j/j+1} \{A_j[\exp(iA_{j+1}\lambda_k) - 1] - A_{j+1}[\exp(iA_j\lambda_k) - 1]\}[A_j A_{j+1}(A_j - A_{j+1})]^{-1}$$

with $A_j = 2\pi \boldsymbol{H}_I \cdot \boldsymbol{e}_j$ and $|\boldsymbol{e}_j| = 1/a_j^*$. Ω_I is the area of the 5D unit cell projected upon $\mathcal{V}_I$, λ_k is the radial atomic-size parameter defined in figure 3. We know from the Patterson analysis that all 5D atoms occupy special positions $(i/5, i/5, i/5, i/5, z)$ i can be an integer between 0 and 4, with minimum site symmetry 5. The same is the case for the original and the general Penrose tilings. Thus it is appropriate to take the general shape of a higher dimensional atom in the case of the general Penrose tiling (cf Pavlovitch and Kléman 1987) for the atomic shapes of the starting model for the least-squares refinements. This corresponds to an irregular decagon with five-fold symmetry defined by the angle $\theta_{j/j+1}$ between the unit vectors $\boldsymbol{e}_j$ and $\boldsymbol{e}_{j+1}$ spanning the decagon (figure 3), and the radius λ_k. In the course of the refinements these shapes changed to regular pentagons and $\theta_{j/j+1}$ has been fixed to the ideal pentagonal value $2\pi/5$. The fine structure of the pentagonal atom of the Penrose tiling, as an example for a possible fine structure in our case, is shown in figure 3(a): each sector corresponds to a particular vertex configuration in the quasicrystal structure and may be occupied by a different atom type. The variation of the Al/Mn ratio for all these different regions would require more parameters than it would be advisable to refine with the given data set. Thus, for each 5D atom, only one

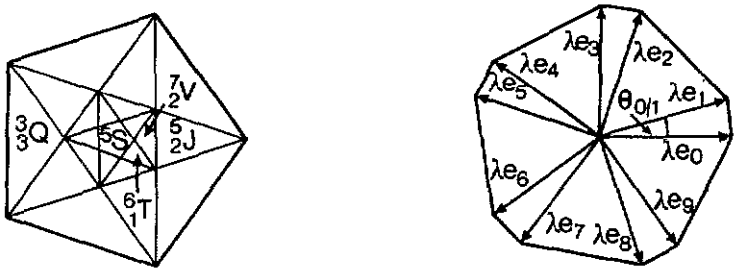

Figure 3. Two examples of possible shapes of the 5D atoms parallel to $\mathcal{V}_\parallel$. Due to the site symmetry the shape has to be invariant under the action of a fivefold rotation. The pentagonal 'atom' drawn in (*a*) corresponds to one of the four 'atoms' generating the original Penrose tiling, the marked regions ('chemical fine structure') correspond to particular vertices of the tiling (cf Pavlovitch and Kléman 1987). The drawing in (*b*) illustrates the shape of 'atoms' in a general Penrose tiling, and is defined by the unit vectors $\boldsymbol{e}_j$ with $j = 0, \ldots, 9$, the radius λ of the circumscribed circle and the angle $\theta_{j/j+1}$ between the unit vectors.

occupational parameter has been refined, giving the ratio of Al to Mn on this site, assuming a statistical distribution over one 5D atom. The internal temperature-factor coefficients adopted values less than their standard deviations and were also reset to zero and fixed.

The refinements smoothly converged to $R = 0.305$ and $wR = 0.144$ for 233 reflections with $I > 2\sigma(I)$ and 18 variables. The quality of the least-squares fit is illustrated by a $F_{obs}(\boldsymbol{H})/F_{clc}(\boldsymbol{H})$ plot in figure 4. Most of the significant deviations from the ideal distribution may result from the bad quality of the metastable Al–Mn crystal leading to rather large systematic errors in the diffraction intensities. Some are due to deficiencies in the structure model since neither the chemical fine structure of the atoms nor the residual electron density appearing in the difference Fourier synthesis (figure 5) have been included in the starting model. The number of parameters would have increased too much for this number of low quality (but the only accessible) reflections. An estimation of the amount of electron density not covered by the refined structure model,

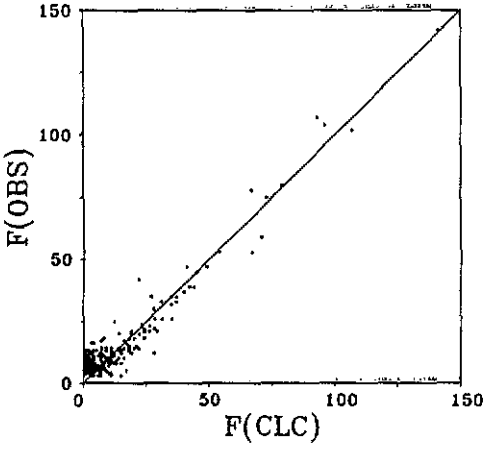

Figure 4. The $F_{obs}(\boldsymbol{H})/F_{clc}(\boldsymbol{H})$ plot for the final model.

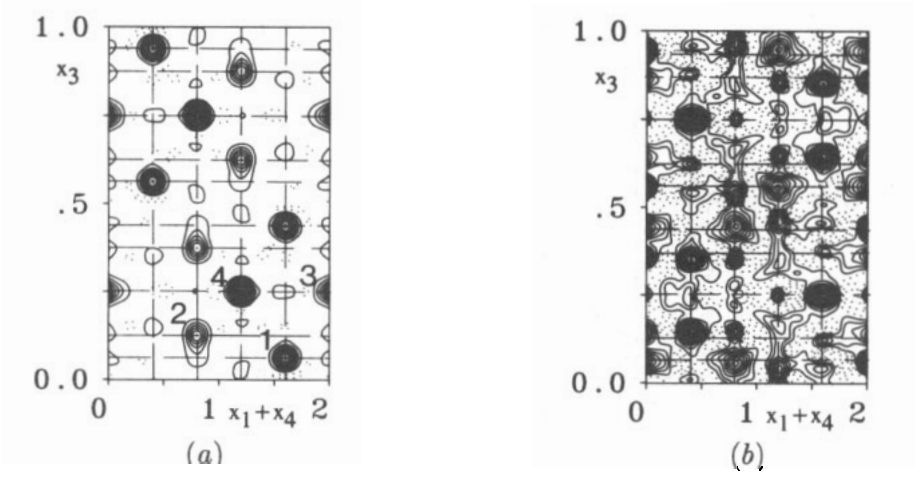

Figure 5. (10110) sections of the 5D (*a*) Fourier (*b*) difference Fourier function calculated after the last refinement cycle from $F_{obs}(H)$ and $F_{obs}(H) - F_{clc}(H)$. The highest maximum in (*b*) is about 12% of the highest one in (*a*). All plot coordinates are given on the v_i basis.

but which results from the Fourier syntheses, comes to a value of about 15%. Though the least-squares fit is not optimal, it can be expected for a centrosymmetric structure that most of the signs of the structure factors are correct, leading to reliable Fourier syntheses and, therefore, to a reliable map of atoms in the decagonal phase.

5. The calculated density

The density of the refined structure model may be calculated in the following way. Each section of a 5D atom with the physical space gives a 3D atom. The probability of such sections is proportional to the area Ω_k^I of the internal component of the nD atom k. For the case when $\Omega_k^I = \Omega^I$ (the projection of the 5D unit cell upon $\mathcal{V}_I$) this probability

Table 1. Parameters of the 5D atoms of decagonal $Al_{78(2)}Mn_{22(2)}$ with ESD's in parentheses. Listed are fractional atomic coordinates x_i (d_i basis), two external (B_{11}^E, B_{33}^E) and one internal (B^I) temperature factor coefficient [Å^2], partial Al site occupancy factor p_{Al} ($p_{Mn} = 1 - p_{Al}$), and radial atomic size parameter λ_k as a fraction of $1/a_i'$. Negative λ_k corresponds to the opposite orientation of the vectors $\lambda_k e_i$.

Parameters	Atom 1	Atom 2	Atom 3	Atom 4
x_1	1/5	3/5	0	2/5
x_2	1/5	3/5	0	2/5
x_3	1/5	3/5	0	2/5
x_4	1/5	3/5	0	2/5
x_5	0.0642(7)	0.123(7)	1/4	1/4
B_{11}^E	1.8(3)	3.0(7)	5(1)	2.4(6)
B_{33}^E	1.7(2)	3.2(6)	2(1)	1.2(4)
B^I	0	0	0	0
p_{Al}	0.84(8)	0.90	0.8(2)	0.3(1)
λ_k	−0.403(2)	−0.356(1)	0.298(2)	0.350(1)

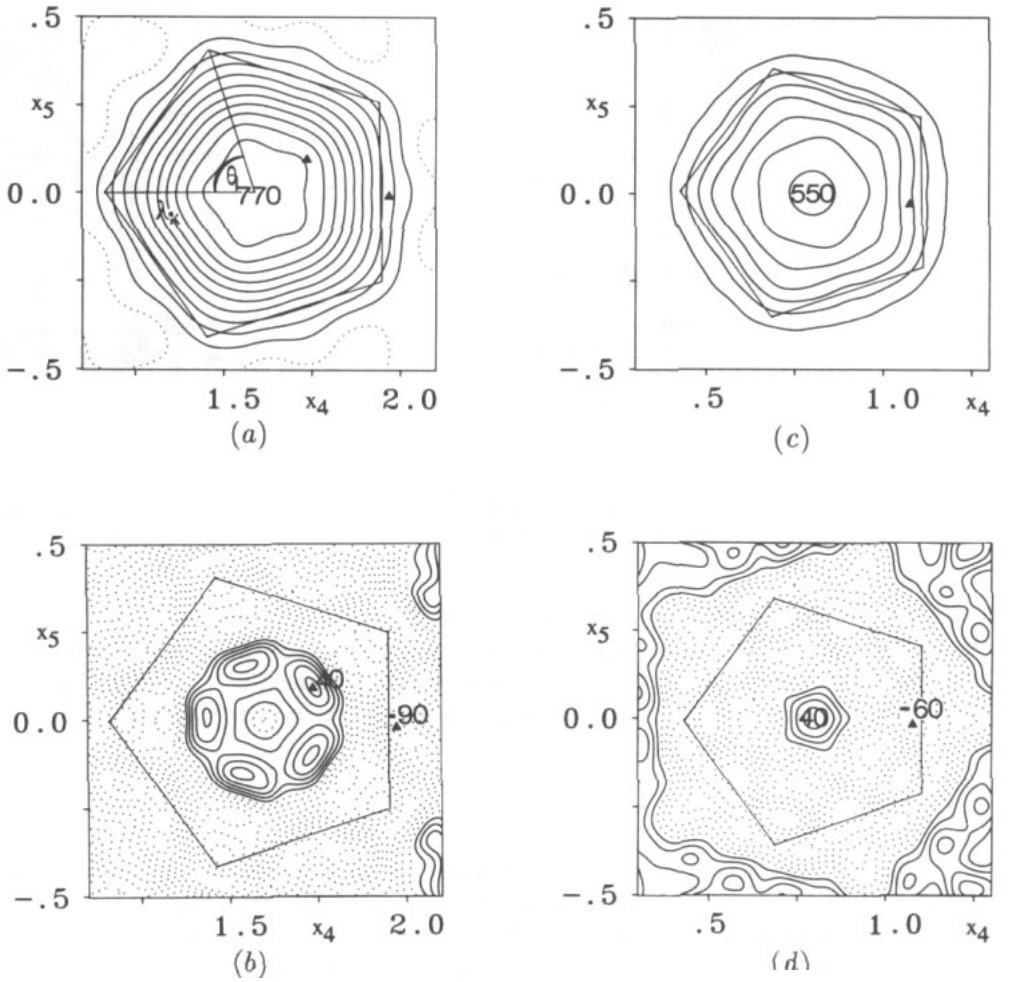

Figure 6. (00011) sections (parallel to the internal space) of the 5D Fourier and difference Fourier functions of respectively, (*a*) and (*b*) atom one, (*c*) and (*d*) atom two, (*e*) and (*f*) atom three, and (*g*) and (*h*) atom four. The refined size parameter λ_k is indicated schematically by the pentagons. Relative peak heights are given in arbitrary units. All plot coordinates are given on the v_i basis.

becomes equal to one. Thus, the ratio Ω_k^I/Ω^I gives the relative frequency of 3D atoms (vertices) generated from the 5D atom k. The number density $\rho_N = (\Sigma\,\Omega_k^I)/\Omega$ (Ω is the volume of the 5D unit cell) gives the number of 3D atoms (vertices) per unit volume. Thus, the density of the quasicrystal can be calculated as $\rho_c = M_r\rho_N/N_L$, where N_L corresponds to the Avogadro number. Inserting the experimental values, we obtain $\rho_c = 3.1\,\mathrm{Mg\,m^{-3}}$. Considering the 15% of additional electron density not included in the refined structure model, one obtains a density of about $\rho_c = 3.6\,\mathrm{Mg\,m^{-3}}$. The density of the decagonal phase has not been measured experimentally, but some values of Al–Mn phases of similar composition are given for comparison: the observed density of icosahedral $Al_{78}Mn_{22}$ is about $3.5\,\mathrm{Mg\,m^{-3}}$ (Yamamoto 1988), of hexagonal φ-$Al_{10}Mn_3$ ($Al_{77}Mn_{23}$) is $\rho_0 = 3.65(5)\,\mathrm{Mg\,m^{-3}}$ (Taylor 1959), of hexagonal μ-$MnAl_4$ ($Al_{80}Mn_{20}$) is

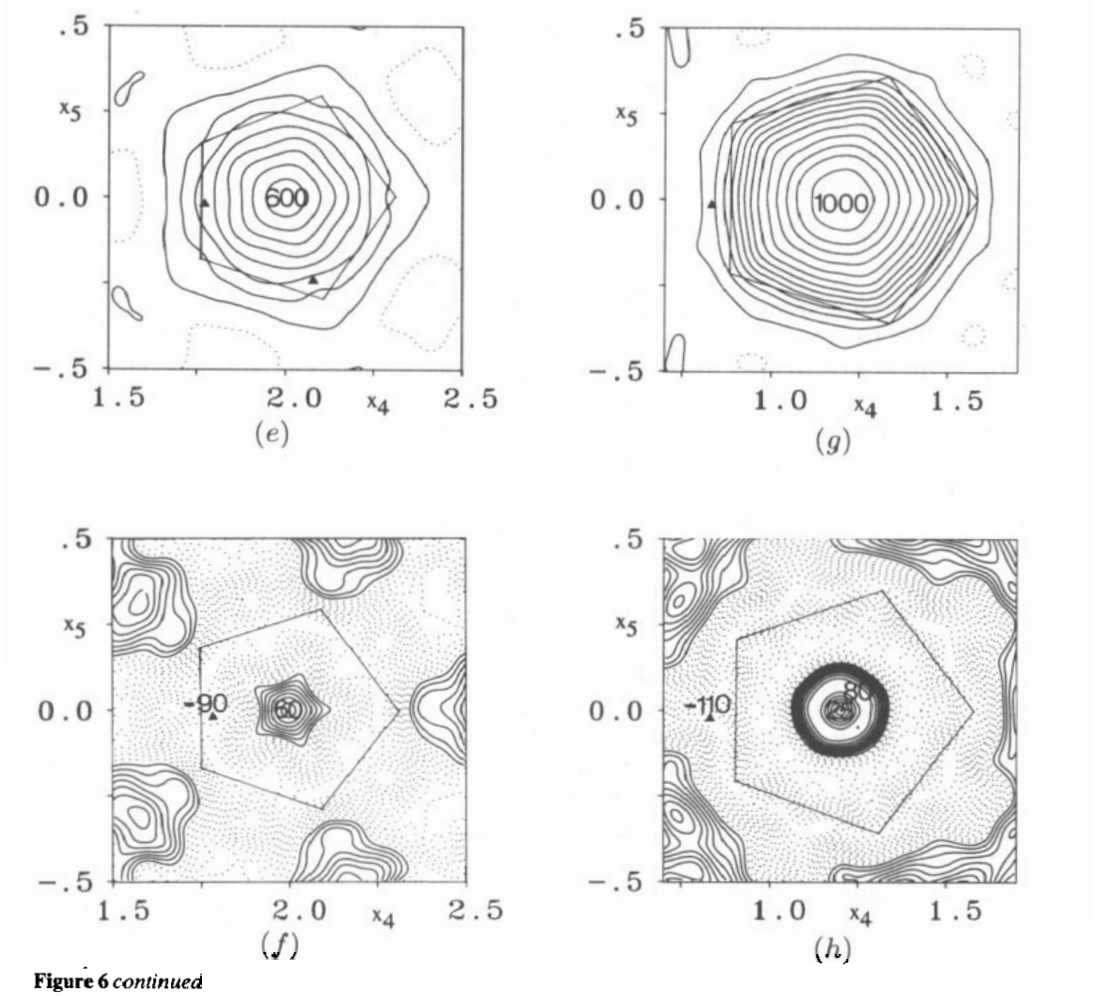

Figure 6 *continued*

$\rho_c = 3.556(2)$ Mg m^{-3} (Shoemaker *et al* 1989), and of triclinic δ-$Al_{11}Mn_4$ ($Al_{73}Mn_{27}$) is $\rho = 3.88$ Mg m^{-3} (Kontio *et al* 1978).

6. Results and discussion

The refined atomic parameters in terms of the 5D description are listed in table 1. All refined atoms occupy special sites ($x_k = i/5$, $i = 0, \ldots, 4$) as is the case for the 2D Penrose tiling. The external thermal parameters (which contain dynamical and static components) are similar to, or slightly higher than, those for atoms of regular structures. The values of the internal temperature factor components give no hints for a significant substitutional disorder in the real quasicrystal structure (phasons). By fixing the Al/Mn ratio of atom 2 to $p_{Al} = 0.9$ during the refinements, the theoretical composition $Al_{78}Mn_{22}$ could be obtained.

The qualitative structure model of Yamamoto and Ishihara (1988) consists of three 5D atoms in the asymmetric unit with positions (−2/5, −2/5, −2/5, −2/5, 0.0833), (−1/5, −1/5, −1/5, −1/5, 0.2500) and (−3/5, −3/5, −3/5, −3/5, 0.2500), given on a different basis however. The atoms have no chemical fine structure and no explicit differentiation between Al and Mn atoms was performed. The structure model only has some basic similarities with the present results.

A more vivid impression about the structure characteristics than can be obtained by numbers can be conveyed by special sections of the 5D Fourier and difference Fourier functions. Thus, the Fourier map of the (10110) plane containing all 5D atoms in the unit cell is given in figure 5(*a*). The maxima marked 1, ..., 4, and their symmetrical equivalents, correspond to the atoms included in the refinements. On the difference Fourier map (figure 5(*b*)) there appear some additional maxima; the maximum peak heights are about 12% of that of atom four in the Fourier map. An integration of the difference density of figure 5(*b*), and of eight more sections parallel to it, yielded an overall residual electron density of 15% of that of the model refined, indicating a lot of disorder. Thus, the four 5D atoms listed in table 1 represent about 85% of the electron density of the quasicrystal, corresponding to the more- or less-ordered part of the structure, while the residual 15%, representative of the disordered part, can be derived from the (difference) Fourier syntheses only. This emphasizes the importance of (difference) Fourier syntheses, a matter of course in regular structure analysis, for a reliable quasicrystal structure determination.

The internal space component of the 5D atoms is characterized in the (00011) sections of the 5D Fourier function (figure 6). The pentagonal shape of the atoms parallel to the internal space is easily recognized. The difference-Fourier plots, giving the electron density resulting from the observed structure amplitudes minus that of the refined model, of figure (6) indicate the chemical fine structure of the 5D atoms. Positive electron density corresponds to a concentration of Mn in this region, negative density indicates more Al relative to the average composition which has been refined for this particular 5D atom. Thus, analogously to figure 3(*a*) each region could be assigned to a particular vertex position occupied by a particular atom. The high degree of disorder (the Fourier synthesis indicates even in these subregions of the 5D atom a statistical Al/Mn distribution) does not let it appear advisable, however, to interpret the chemical fine structure in a more detailed way. The position of each type of atom in the 3D real structure can be seen much more easily in the Fourier sections of figures 7 and 8.

7. The structure of the layers

In figure 7, large real space (11000) sections of about 23.5 × 23.5 Å^2 of the 5D Fourier function are shown with line drawings illustrating the characteristical features. For sake of clarity the (10010) sections are also given in each case. The correspondence of 3D and 5D maxima becomes more transparent in this way as do the global differences between the different layers. In figure 7(*a*) and (*b*) the highest maxima are connected in such a was as to show the close resemblance of these two layers, which may be considered as *one* corrugated layer, with the puckered ($y = \frac{1}{4}$) layer of crystalline $Al_{13}Fe_4$ (cf figure 4 of Black 1955). As for $Al_{13}Fe_4$, this layer consists primarily of Al. In the (10010) section one unit cell containing the atoms one and two is marked in each case. The broken lines corresponds to the lines at $x_3 = 0.064$ and 0.124 in figure 5(*a*). Henley (1985) and Kumar

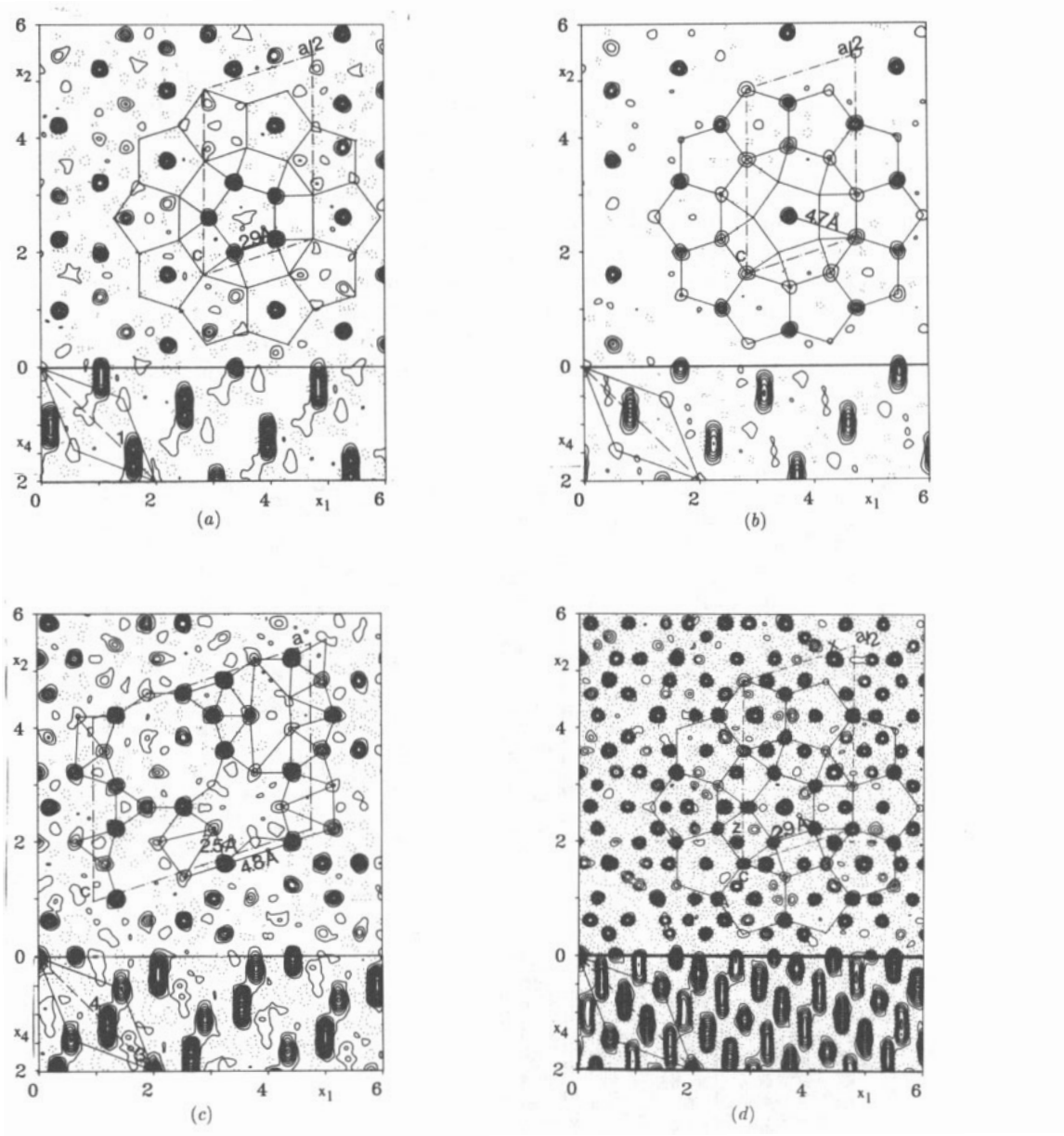

Figure 7. Quasiperiodic (11000) sections (parallel to the external space with a size of about 23.5 × 23.5 Å^2) of the 5D Fourier function of decagonal $Al_{78}Mn_{22}$ at (*a*) $x_3 = 0.064$, (*b*) $x_3 = 0.124$ and (*c*) $x_3 = \frac{1}{4}$. Characteristic structure motifs are marked, which can also be found in slightly distorted form in the $Al_{13}Fe_4$-type structures. (*d*) The quasicrystal structure projected down the tenfold screw axis (calculated from reflections $F(h_1, h_2, h_3, h_4, 0)$, only). Additionally, the respective (10010) sections are shown to allow visualization of the correspondence between 5D and 3D structures. All plot coordinates are given on the v_i basis.

et al (1986) already pointed out that the puckered layer of the $Al_{13}Fe_4$ structure may be considered as a relaxed decorated 2D Penrose tiling.

In figure 7(*c*) the maxima are connected differently to emphasize the close resemblance of the $x_3 = \frac{1}{4}$ layer with the plane ($y = 0$) layer of crystalline $Al_{13}Fe_4$ (cf figure 3 of Black 1955). The unit cell of $Al_{13}Fe_4$ is marked with a chain line. Despite small shifts and a slightly different distribution of Al and transition metal atoms (the strong maxima in this Fourier section correspond to Mn atoms), these structure elements appear to be the same in both phases. The ratio of transition metal to aluminium in this layer is higher than that for the corresponding $Al_{13}Fe_4$ layer.

The distances between strong maxima (Mn–Mn) of about 4.8 Å agree quite well with the pair distances resulting from the neutron contrast variation study of Dubois and Janot (1988); the same is true for Mn–Al and Al–Al distances.

The projection of the structure upon (11000) (Fourier synthesis calculated with $F(h_1h_2h_3h_40)$, only) is given in figure 7(*d*). It shows the same structural characteristics

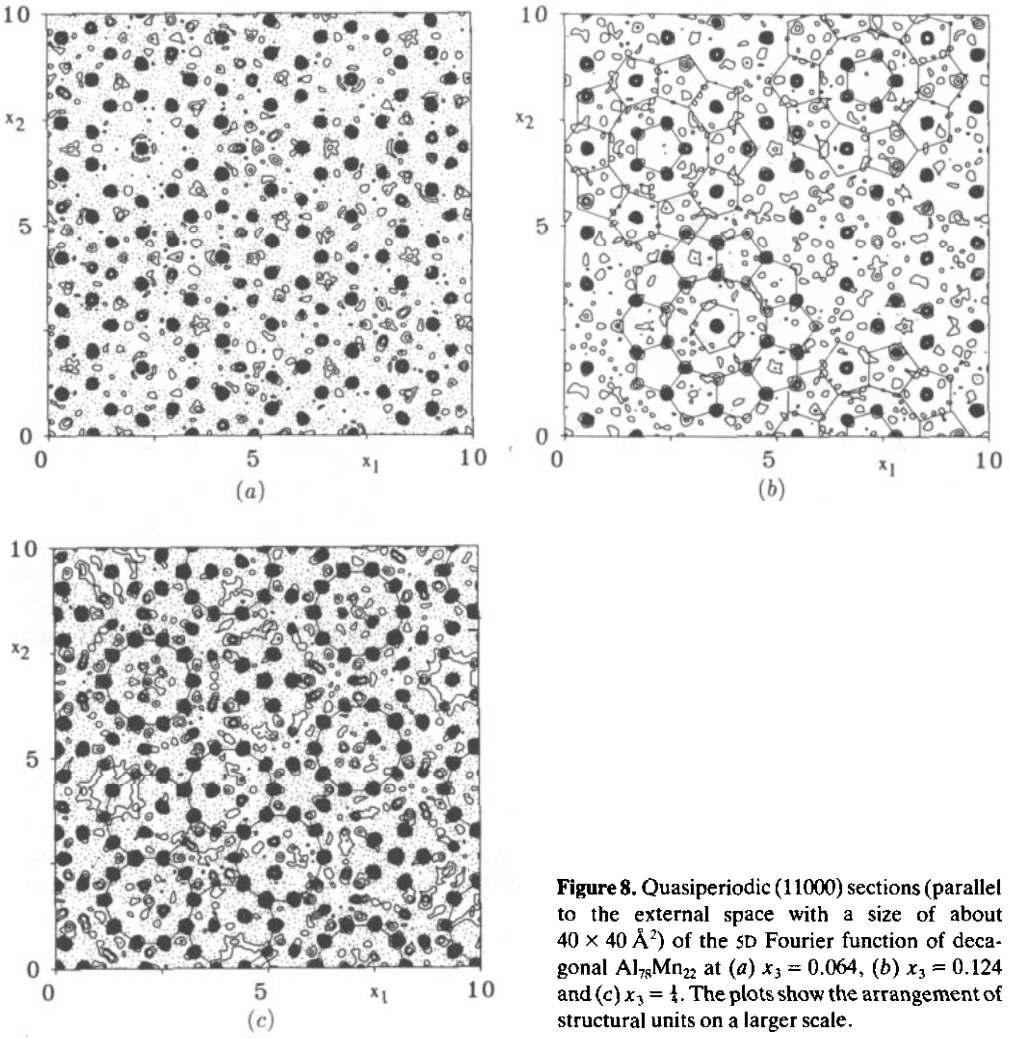

Figure 8. Quasiperiodic (11000) sections (parallel to the external space with a size of about 40×40 Å^2) of the 5D Fourier function of decagonal $Al_{78}Mn_{22}$ at (*a*) $x_3 = 0.064$, (*b*) $x_3 = 0.124$ and (*c*) $x_3 = \frac{1}{4}$. The plots show the arrangement of structural units on a larger scale.

as the analogous map for decagonal $Al_{65}Cu_{20}Co_{15}$ (Steurer and Kuo 1990). The only difference is that in the present case the pentagonal channels parallel to the tenfold screw axis are all occupied: the occupation is not in alternating manner. This also shows good agreement with structure motives visible on a HRTEM image of decagonal Al–Mn published as figure 8 by Hiraga *et al* (1987).

Larger sections (of about 40×40 Å^2) of the electron density maps of the three different layers are given in figure 8 to illustrate the distribution of the decagonal and pentagonal structure motifs.

8. The layer structure

The 3D decagonal structure results from stacking sandwiches, each one consisting of one planar layer ($x_3 = \frac{1}{4}$; one has to keep in mind that the coordinate of the periodic axis corresponds to x_3 on the $\boldsymbol{v}_i$ basis and to x_5 on the $\boldsymbol{d}_i$ basis, respectively) between two symmetrically equivalent puckered quasiperiodic layers (those containing the atoms with $x_3 = 0.064$ and $x_3 = 0.124$, as well as $x_3 = 0.436$ and $x_3 = 0.376$). These sandwiches are rotated by 36° relative to one other. The distances between the atoms of these two symmetrically equivalent layers should correspond to the frequent distances found for the pair correlation function (Dubois and Janot 1988). This can easily be verified for the atoms in the layers with $x_3 = 0.064$ and $x_3 = \frac{1}{2} - 0.064$ with a spacing of 4.66 Å, but not for the layers in $x_3 = 0.124$ and $x_3 = \frac{1}{2} - 0.124$. The resulting distance of 3.1 Å does not appear in the table of pair distance functions. This dilemma, however, can be overcome by looking at figure 5(*b*). The 5D difference Fourier map clearly shows, that the 5D atom two in reality is split into two atoms, one centred on the first atom layer with $x_3 = 0.064$, and the other at about $x_3 = 0.14$. The resulting spacing between symmetrically equivalent atoms of about 2.7–2.8 Å can be related to the observed pair distances again.

The 3D coordination polyhedra are almost the same as those occurring in the $Al_{13}Fe_4$ structure (cf figure 1 of Black 1955), thus, the same is true for the distances. What are now the principal structural differences between both the quasiperiodic and the related periodic $Al_{11}Fe_4$ phases? Both have a preference for the formation of planar pentagonal and decagonal structure elements; they differ primarily in the way in which these structure elements are combined. The puckered ($y = \frac{1}{4}$) crystalline layer consists of infinite wavy bands of edge-connected pentagons running parallel to $\boldsymbol{a}$. In the case of the quasiperiodic puckered ($x_3 = 0.064 + 0.124$) layer, ten of these pentagons are arranged in the form of decagonal rings centred by a further pentagon. The crystalline plane ($y = 0$) layer shows dimers of unregular decagons like holes in a network of infinite chains of edge-connected triangles running parallel to $\boldsymbol{c}$ and to $\boldsymbol{a} + \boldsymbol{c}$, respectively. In the corresponding quasicrystalline layer these decagons become regular and appear isolated or in pentagonal clusters. In both cases the quasiperiodic arrangement allows the formation of undistorted regular pentagons and decagons that may be favourable energetically.

9. Summary

The aim of the present study was to obtain a model of the 3D structure of decagonal $Al_{78(2)}Mn_{22(2)}$. Practically, this can only be performed via 3D Fourier syntheses. The prerequisite for these calculations is the knowledge of the signs of the structure factors.

The main objective of our 5D least-squares structure refinement was, therefore, to obtain the signs. Even for the moderate R-factor of 0.144, one can expect correct signs for most of the structure factors, since for a change of the sign the magnitude of a structure factor had to run through zero. The electron density maps indicate a close resemblance of $Al_{78(2)}Mn_{22(2)}$ with the crystalline $Al_{11}Fe_4$ structure, and similar coordination polyhedra with comparable distances consequently occur. In contrast to decagonal $Al_{65}Cu_{20}Co_{15}$, which is a two layer structure, decagonal $Al_{78(2)}Mn_{22(2)}$ is built of six quasiperiodic layers.

References

Black P J 1955 *Acta Crystallogr.* **8** 175–82

Dubois J M and Janot C 1988 *Europhys. Lett.* 5 235–40

Henley C L 1985 *J. Non-Cryst. Solids* **75** 91–6

Hiraga K, Hirabayashi M, Inoue A and Masumoto T 1987 *J. Microscopy* **146** 245–60

Janssen, T 1986 *Acta Crystallogr.* A **42** 261–71

Kontio A, Stevens E D, Coppens P, Brown R D, Dwight A E and Wiliams J M 1978 *Acta Crystallogr* B **36** 435–6

Kumar V, Sahoo D and Athithan G 1986 *Phys. Rev.* B **34** 6924–32

Levitov L S and Rhyner J 1988 *J. Physique* **49** 1835–49

Pavlovitch A and Kléman M 1987 *J. Phys. A: Math. Gen.* **20** 687–702

Prince E 1982 *Mathematical Techniques in Crystallography and Materials Science* (New York: Springer) p 94–8

Shoemaker C B, Keszler D A and Shoemaker D P 1989 *Acta Crystallogr* B **45** 13–20

Steurer W 1989 *Acta Crystallogr.* B **45**, 534–42

Steurer W 1990 *Z. Kristallogr.* **190** 179–234

Steurer W and Kuo K H 1990 *Acta Crystallogr* B **46** 703–12.

Steurer W and Mayer J 1989 *Acta Crystallogr* B **45** 355–9

Taylor M A 1959 *Acta Crystallogr.* **12** 393–6

deWolff P M 1974 *Acta Crystallogr.* A **30** 777–85

Yamamoto A 1988 *Phys. Rev* B **37** 6207–14

Yamamoto A and Ishihara K N 1988 *Acta Crystalogr* A **44** 707–14